Three-dimensional flow in cavities

By D. J. MAULL AND L. F. EAST
Engineering Laboratory, University of Cambridge

(Received 18 January 1963)

The flow inside rectangular and other cavities in a wall has been investigated at low subsonic velocities using oil flow and surface static-pressure distributions. Evidence has been found of regular three-dimensional flows in cavities with large span-to-chord ratios which would normally be considered to have two-dimensional flow near their centre-lines. The dependence of the steadiness of the flow upon the cavity's span as well as its chord and depth has also been observed.

1. Introduction

Preparatory to an investigation into the fluctuating pressures in a two-dimensional cavity, oil flow tests were carried out on a cavity to check that a sufficiently large aspect ratio had been chosen to give flow over the central region which was sensibly two-dimensional. It was immediately apparent that the flow was not two-dimensional anywhere in the cavity but was instead of a regular three-dimensional nature. Although no reference has been found concerning this effect, the oil flow patterns given by Plumblee, Gibson & Lassiter (1962) for cavities for which the span was 2 in., the depth 2·5 in. and the chords were 1 and 2 in., reveal possible evidence of its existence at supersonic speeds, though the small size of the photographs makes detailed analysis difficult.

2. Experimental arrangement

The experiments were carried out in three different low-speed wind tunnels. Initially a rectangular cavity of span $S = 19$ in., chord $b = 4$ in. and depth $d = 2$ in. was mounted in the top of a closed return wind tunnel having a working section of 32×28 in. and a maximum air velocity of about 90 ft./sec (figure 1). The free-stream dynamic pressure q was measured by the use of a Pitot-static tube set at the centre of the working section.

The second series of experiments, which yielded the quantitative information concerning rectangular cavities, used a cavity of span 18 in., chord 2 in. and depth variable from zero to 6·8 in., by means of a piston arrangement as shown in figure 2, mounted in the side of an open return tunnel having a working section of $20 \times 7\frac{1}{2}$ in. and a maximum flow velocity of 250 ft./sec. As before the dynamic pressure was measured using a Pitot-static tube at the centre of the working section. The wall boundary-layer profile approaching the cavity is shown in figure 3 for a free-stream velocity U of 200 ft./sec, which was the nominal velocity at which the majority of readings were taken. Reference is also made to some preliminary tests done in this tunnel using a cavity of span 13 in.,

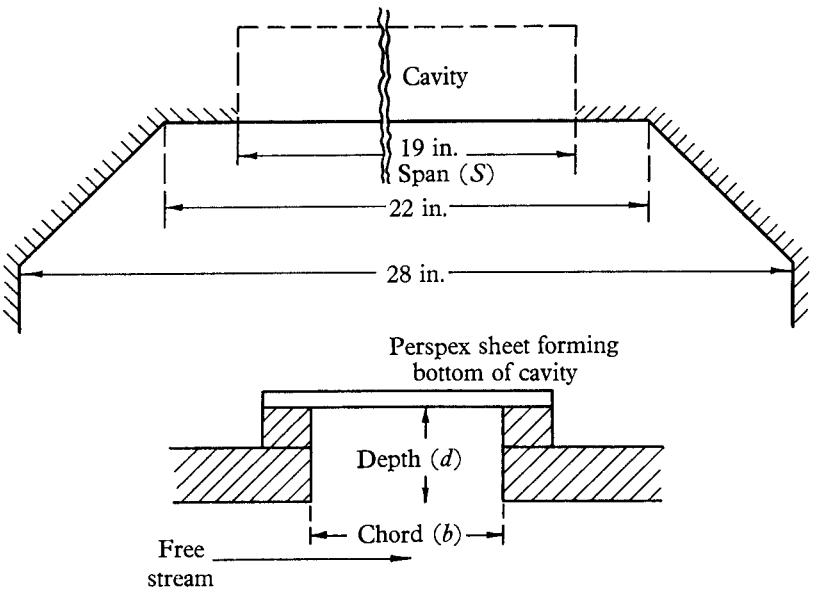

FIGURE 1. Rectangular cavity mounted in top of closed return tunnel.

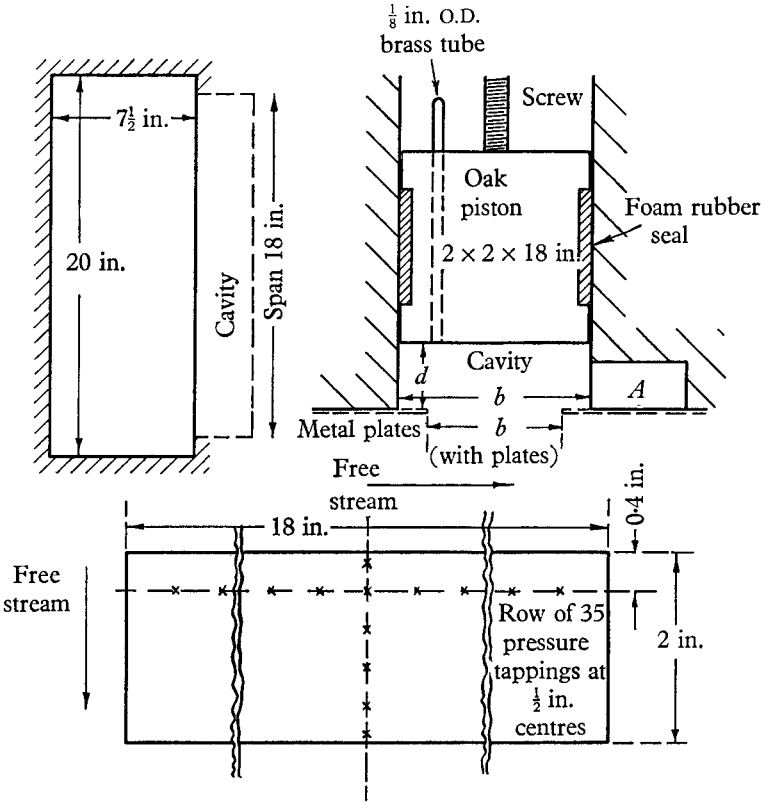

FIGURE 2. Variable depth rectangular cavity with details of piston and pressure tappings.

chord $2\frac{3}{4}$ in. and depth variable from zero to 4 in. However, difficulty was experienced in sealing the piston and it was superseded by the cavity mentioned above.

Tests with cavities of circular cross-section were carried out in an open return wind tunnel, having a working section of 20 × 28 in. and a maximum air velocity of about 140 ft./sec. The cavities, which were formed from a brass tube of internal diameter 1·54 in. and length 10 in. as shown in figure 4, were mounted in the bottom of the working section. The dynamic pressure in this case was determined from the static pressure difference across the upstream contraction and the tunnel calibration constant.

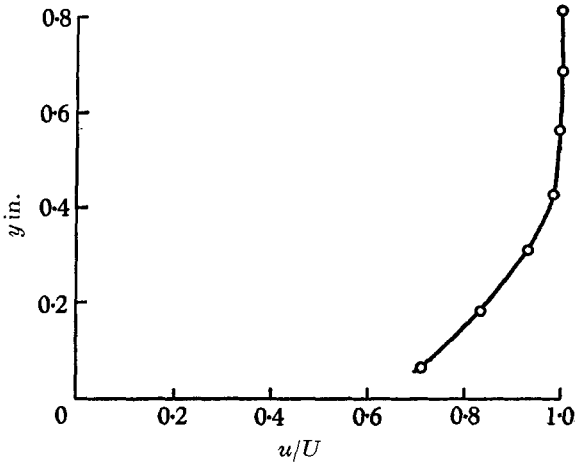

FIGURE 3

3. Experimental procedure and observations

Evidence of three-dimensional effects was first obtained by the use of the oil flow visualization technique on the 'bottom' of the cavity shown in figure 1. By using a Perspex bottom to the cavity and a thin film of oil it was possible to view and photograph the oil patterns obtained from outside the tunnel while it was running.

The flow in a two-dimensional cavity probably has the general form shown in figure 5, and it would be expected that if the flow over the central portion of the span were two-dimensional the collection of oil indicating the separation line on the bottom of the cavity would appear straight.

Figure 6*a* shows the first oil pattern produced, of which two features are noteworthy. First, the spanwise line of separation on the bottom of the cavity is not straight even near the tunnel centre but appears to form a regular wave, and secondly, it is not symmetrical about the centre line. By inserting wooden blocks the span was reduced by steps down to 6 in. and this procedure showed that the flow breaks down into a series of cells, each containing three-dimensional flow and each a mirror image of those adjacent to it. The span s of each cell was in this case a little less than the chord and remained essentially independent of the total cavity span. The effect of changing the total span is primarily to change the number of cells, as is shown in figures 6*a–c*, plate 1, which have 5, 4 and 3 cells, respectively. It was not found possible to obtain an oil flow pattern which gave the details of the flow at all points on the bottom in one photograph, but figures

6*b* and *c*, plate 1, together give a good indication. In the original photograph of figure 6*b* considerable detail of the flow leaving the downstream wall can be seen and in particular the fanning out of the streamlines from the centre and from the ends of the cavity is clear. Figure 6*c* was obtained with very little oil and therefore gives some indication of the flow in the vicinity of the separation line. It appears to suggest the presence of a row of vortices, in this case three, having their axes normal to the bottom of the cavity and terminating on it. Figure 7, which is based on the oil flow photographs, shows the probable surface streamlines on the bottom of the cavity.

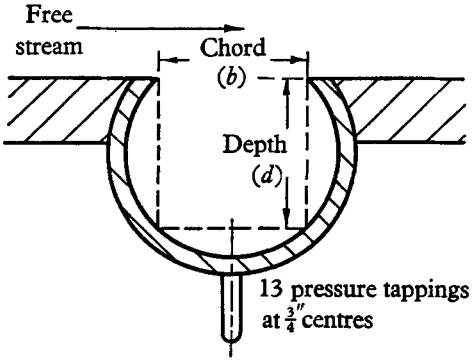

FIGURE 4. Circular cavity.

It is evident that there are two possible configurations for any series of cells, the second being obtained from the first by inverting each cell about its centre line (figure 7). In a cavity containing an odd number of cells the second configuration will be equivalent to inverting the whole flow about the cavity centre line, but in the case of an even number of cells this is clearly not so, and in particular a different centre line pressure distribution will result. Both these inversions were noted during the oil flow tests and figure 8, plate 2, shows a series of photographs of a four-cell configuration which underwent such a change. It will be seen that between figure 8*b* and *c* an inversion must have taken place, for figure 8*c* shows the oil adapting itself to the new flow conditions which have almost been reached in figure 8*d*.

The presence of three-dimensional flow posed the question as to whether the static-pressure distribution on the bottom of the cavity was consequently modified by a significant amount. To investigate this the Perspex 'bottom' was replaced by a brass plate fitted with 70 static pressure tappings as shown in figure 9. It was found that the spanwise static pressure distribution is affected by the cell structure, as shown in figure 10, and consequently the chordwise pressure distributions are affected by their spanwise position as is also indicated in figure 11. The magnitude of the variation of the pressure coefficient C_p may appear insignificant but this is a result of the convenience of basing C_p on the free-stream dynamic pressure rather than on a representative dynamic pressure within the cavity. Since the maximum velocity within the cavity is about one-third of the free-stream velocity the pressure coefficient based upon the former would be about ten times as great as the values presented.

The correlation between the spanwise static pressure distributions and the oil flow photograph suggests that to ascertain the presence and size of cells in a variety of cavity configurations the former method is adequate, and on account of its ease of application no further use was made of the oil flow visualization technique in subsequent tests.

To provide further information about the formation of cells experiments were carried out on the cavity shown in figure 2 at a nominal free-stream velocity of 200 ft./sec, except where otherwise specified in the text.

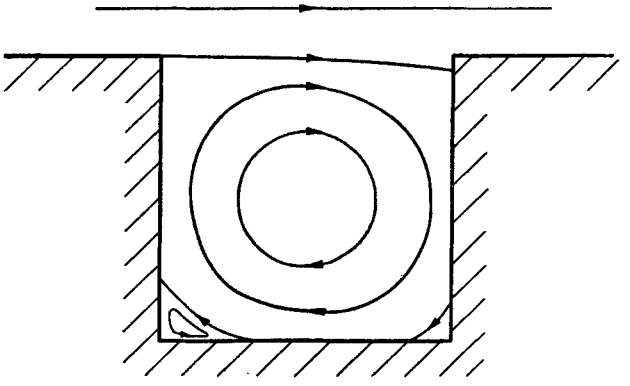

FIGURE 5. Streamlines in two-dimensional cavity.

4. The effect of varying the cavity span and depth

The characteristics of the spanwise static-pressure distribution were observed as the ratio d/b was varied, the ratio S/b being kept constant at 9·0. It was found that for values of d/b less than 0·45 the spanwise pressure distribution showed no sign of any wave formation, though as is to be expected end effects were present. However, at $d/b = 0{\cdot}45$ a wave structure first appeared which grew in amplitude without change in wavelength as d/b approached 0·5 (figure 12). As d/b was further increased the wavelength changed discontinuously, being governed by the condition that there be an integral number of cells in the total span. Under these conditions, dictated by a finite span, an intermediate value of d/b produced a distorted wave structure of diminished and usually time-dependent amplitude. At a value of $d/b = 0{\cdot}875$ for the cavity in which $S/b = 9{\cdot}0$, also at a value of $d/b = 0{\cdot}91$ in the preliminary tests in which $S/b = 4{\cdot}73$, a sudden change occurred from a steady wave formation to apparent two-dimensional flow. The exact value of d/b at which this change occurs depended upon S/b. While d/b was further increased to a value of about 1·2 the distribution remained two-dimensional. At $d/b = 1{\cdot}2$, waves started to build up, and for values of d/b between 1·25 and 1·52 the distribution appeared as moving waves whereas the change from 1·52 to 2·05 was achieved by distorting the waves but was at no time unsteady. Above $d/b = 2{\cdot}05$ the wave formation diminished and at $d/b = 2{\cdot}5$ a two-dimensional configuration appeared to be present. This remained up to the limit of the experiment at $d/b = 3{\cdot}4$, except that between $d/b = 3{\cdot}3$ and $d/b = 3{\cdot}4$ one end of the distribution became distorted; it was, however, impossible to tell whether this was an end effect or the start of a wave formation.

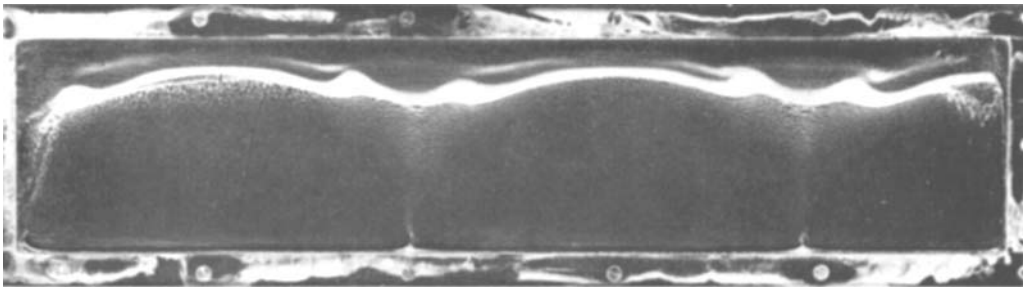

(*a*)

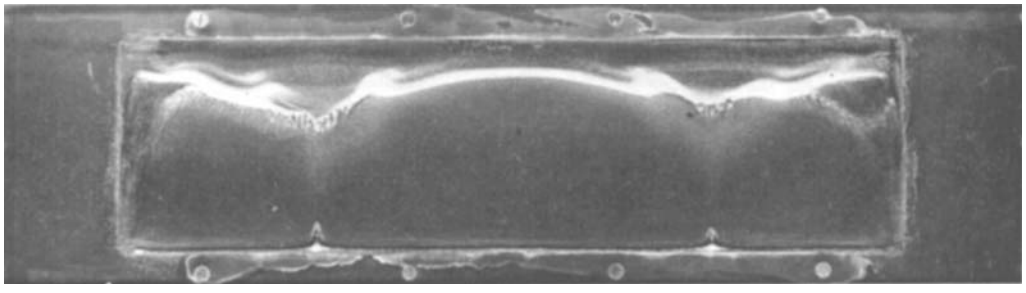

(*b*)

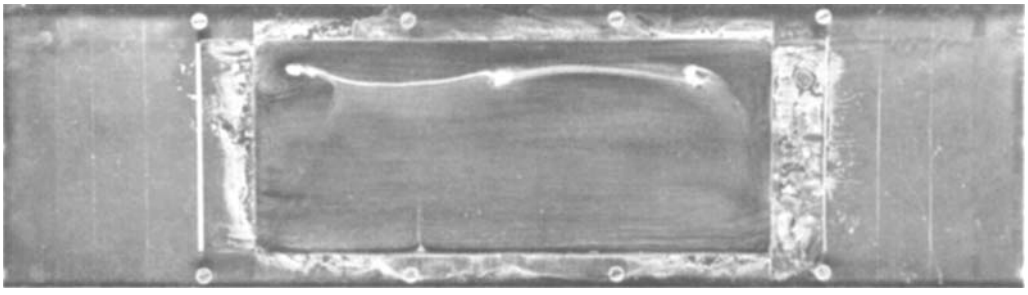

(*c*)

FIGURE 6. Oil patterns, with free-stream direction from top to bottom of page. (*a*) Span 19 in., (*b*) span 15 in., (*c*) span 10 in.

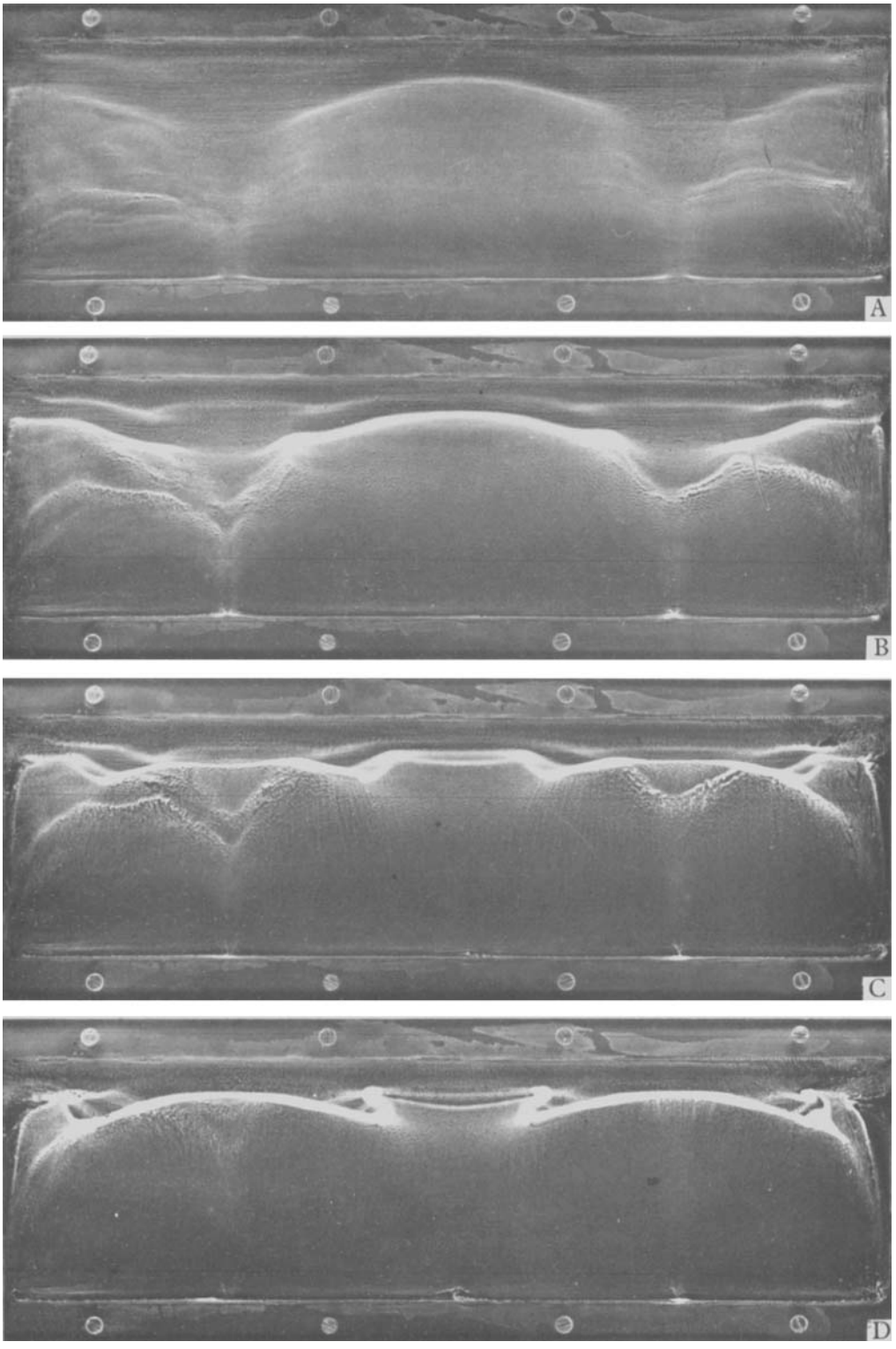

FIGURE 8. Sequence of oil patterns showing change of cell arrangements, $d/b = 0{\cdot}5$, $S/b = 3{\cdot}75$. Free-stream direction from top to bottom of page.

It appears from the above tests that a cell has a preferred span which is a function of the chord and the depth of the cavity. This span can be compressed or expanded to only a limited extent and hence the cell formation is dependent upon the total span in so far as the steadiest and most regular conditions are

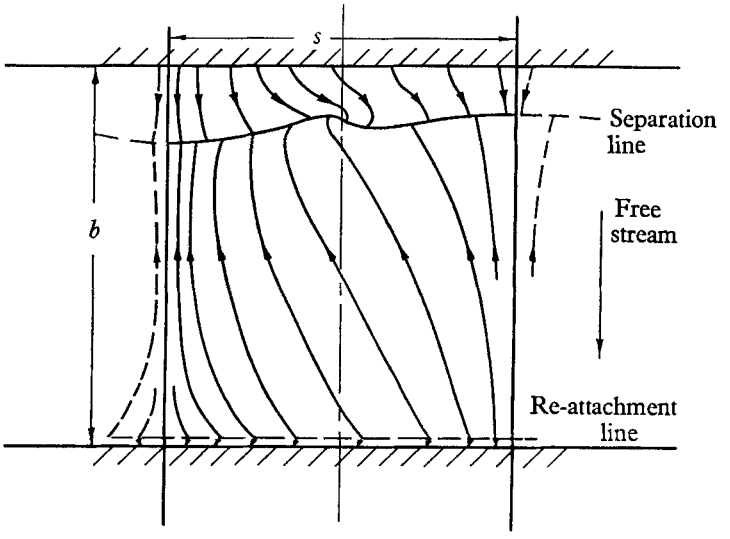

FIGURE 7. Surface streamlines on the bottom of cavity within one cell $d/b = 0{\cdot}5$.

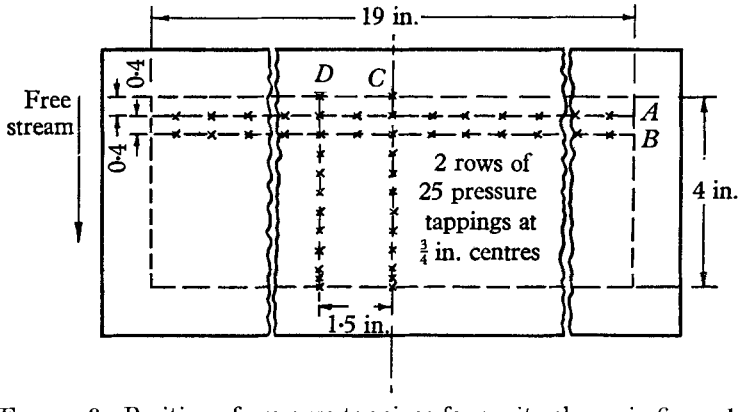

FIGURE 9. Position of pressure tappings for cavity shown in figure 1.

obtained only when the total span is an integral number of cell spans. To investigate this further S/b was varied while d/b was kept constant at 0·5. The span was varied by the insertion of wooden blocks of suitable sizes, and although the cavity was sealed from the air outside the tunnel, it was not found possible to seal the periphery of the blocks satisfactorily, and thus the spanwise pressure distribution is continuous over the complete span. This introduces the end condition for blocked-in cavities that the pressure towards the end of the cavity shall tend towards the pressure on the underside of the block. This effect can be seen in figure 13 and while it alters the detailed shapes of the curves it does not appear to have affected the basic cell formation. In figure 13 are shown some of

It appears from the above tests that a cell has a preferred span which is a function of the chord and the depth of the cavity. This span can be compressed or expanded to only a limited extent and hence the cell formation is dependent upon the total span in so far as the steadiest and most regular conditions are

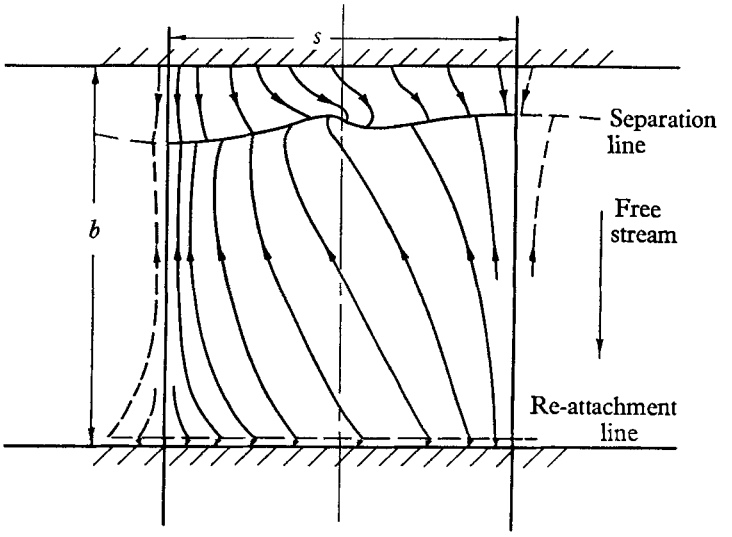

FIGURE 7. Surface streamlines on the bottom of cavity within one cell $d/b = 0{\cdot}5$.

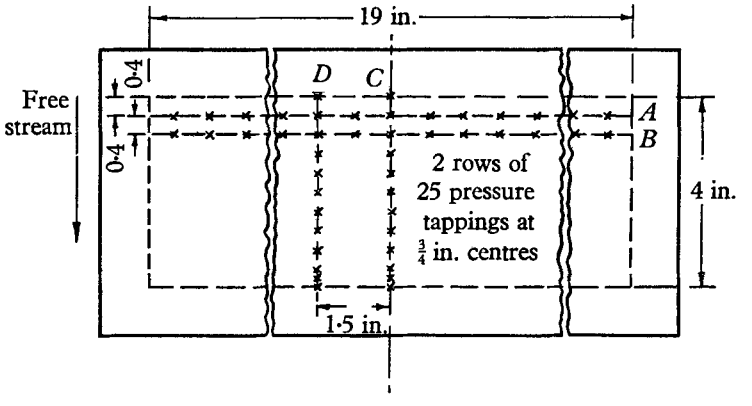

FIGURE 9. Position of pressure tappings for cavity shown in figure 1.

obtained only when the total span is an integral number of cell spans. To investigate this further S/b was varied while d/b was kept constant at 0·5. The span was varied by the insertion of wooden blocks of suitable sizes, and although the cavity was sealed from the air outside the tunnel, it was not found possible to seal the periphery of the blocks satisfactorily, and thus the spanwise pressure distribution is continuous over the complete span. This introduces the end condition for blocked-in cavities that the pressure towards the end of the cavity shall tend towards the pressure on the underside of the block. This effect can be seen in figure 13 and while it alters the detailed shapes of the curves it does not appear to have affected the basic cell formation. In figure 13 are shown some of

those pressure distributions which were found to be steady, while other values of S/b tested gave pressures which were strongly time dependent. From these tests it appears that the non-dimensional cell span s/b can vary very little for a given value of d/b, and for the particular case of $d/b = 0{\cdot}5$ reasonable limits of s/b may be 0·88 and 0·93.

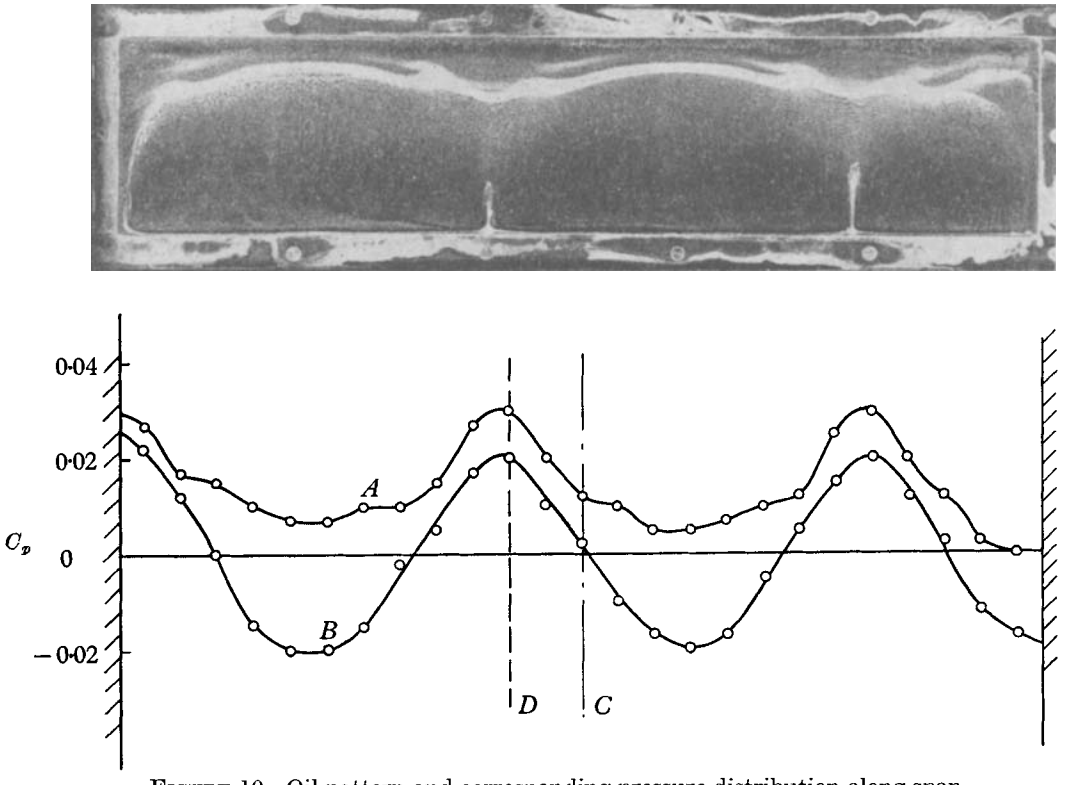

FIGURE 10. Oil pattern and corresponding pressure distribution along span.

The centre-line pressure distributions corresponding to the above configurations demonstrate their dependence upon S/b. For those values of S/b which produced steady conditions above, the centre-line pressure distributions were also steady though they differed from one another. The remaining values of S/b used produced centre-line distributions which varied greatly with time, particularly in the region of the downstream wall of the cavity.

5. The effect of rounding the downstream corner

The cavity was next modified by rounding the downstream corner A in figure 2 such that $r/b = 0{\cdot}25$, where r is the radius of curvature of the corner, and d/b was then varied as before. The general effect of the radius is to increase the stability of the flow with respect to time and to reduce the amplitude of the wave pattern of the transverse pressure distribution to about a quarter of that obtained under similar conditions in the absence of the radius on the downstream corner. No configuration with an odd number of cells appeared to be obtainable at a

free-stream velocity of 200 ft./sec. On increasing d/b a reasonably stable configuration was obtained at $d/b = 0{\cdot}5$, which was of similar amplitude to the case without the radius but much distorted. At $d/b = 0{\cdot}85$ an eight-cell configuration was obtained which was the most regular of the series. The change from the $d/b = 0{\cdot}5$ configuration to that at $d/b = 0{\cdot}85$ was made steadily and at a reduced amplitude. Above $d/b = 0{\cdot}85$ the cell structure suddenly vanished, as before, and as can be seen in figure 14 a two-dimensional distribution was obtained.

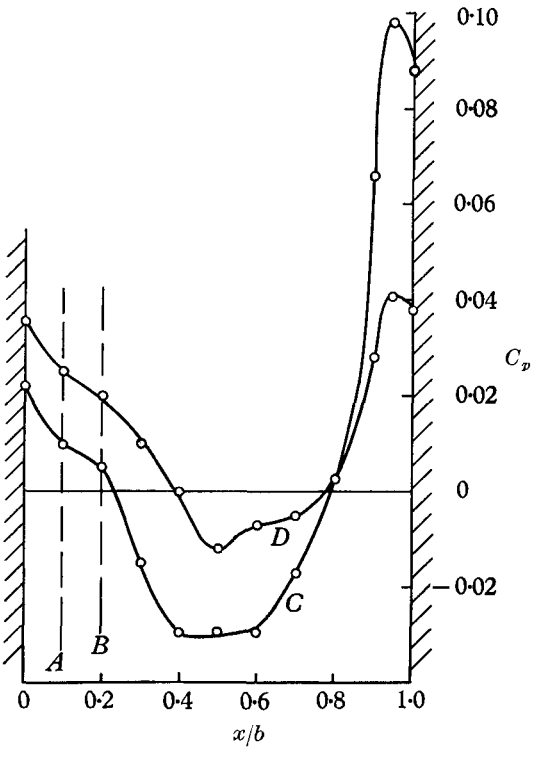

FIGURE 11. Pressure distribution along the chord corresponding to oil pattern of figure 10.

Above $d/b = 0{\cdot}86$ no regular configurations were obtained at $U = 200$ ft./sec; the pressure distribution being of small amplitude (C_p range of about 0·01) and generally having a fairly steady wave at one end and progressively becoming more unsteady and distorted towards the other. It was found, however, that by raising the velocity to 250 ft./sec, a regular stable five-cell configuration could be obtained at $d/b \simeq 2{\cdot}0$, which suggests that the effect is dependent upon the ratio of the boundary layer thickness to the cavity breadth or the Reynolds number or both.

6. The effect of reducing the cavity breadth by projecting plates

The cavity was fitted with two metal plates, each of thickness 0·036 in., placed so as to form a centrally positioned gap of 1·42 in., as shown in figure 2. The ratio d/b was then varied as before.

In general it was found that the effect of the plates was similar to that of the rounded corner in that the amplitude was reduced to about a quarter of the normal rectangular case. For very shallow cavities, as before, the flow was found to be sensibly two-dimensional, but in the region of $d/b = 0{\cdot}4$ waves started to form at the ends and remained up to about $d/b = 0{\cdot}6$. Although the waves were moderately stable it was not found possible to obtain a regular wave formation across the whole span, as in the case of $d/b = 0{\cdot}5$ for the open rectangular cavity.

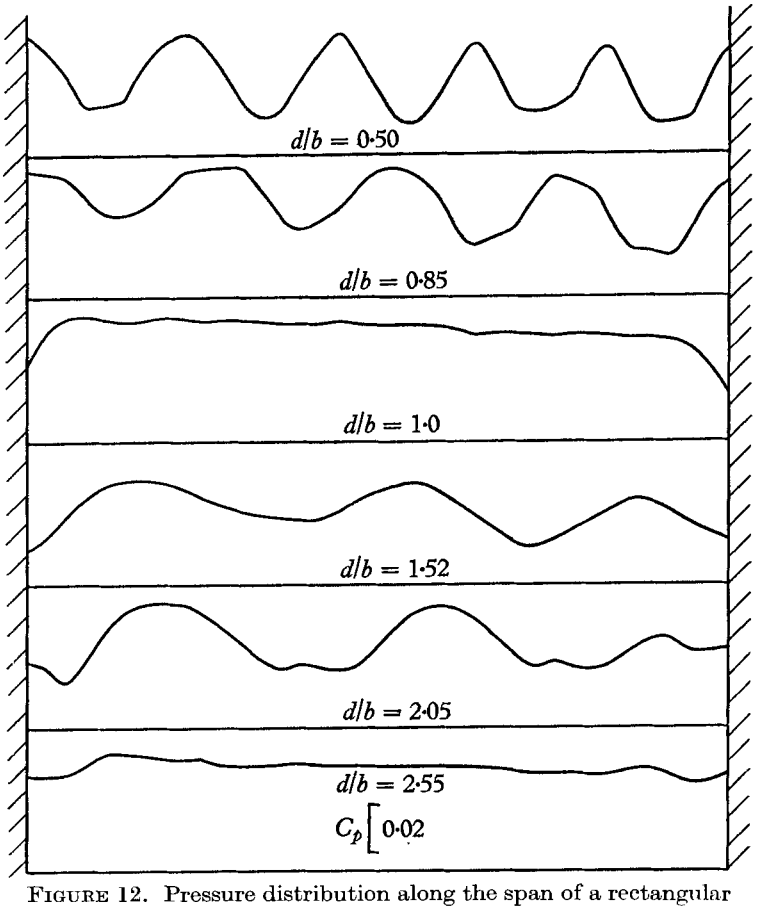

FIGURE 12. Pressure distribution along the span of a rectangular cavity for varying d/b, $S/b = 9{\cdot}0$.

Above $d/b = 0{\cdot}4$ no two-dimensional régimes were obtained, even for a 'square' cavity and small amplitude unsteady waves were always present. The only steady waves obtained were for $d/b \simeq 1{\cdot}9$ and between 2·35 and 2·7, but in both cases the pressure distribution changed very little with depth, except that at $d/b = 2{\cdot}08$ a sudden change between the two configurations occurred at large amplitude (C_p range of about 0·04).

7. Circular cavities

Two cavities were tested having circular cross-sections as shown in figure 4. This was thought expedient for although no theoretical analysis is put forward

in this report it seems reasonable to expect that the simplest configuration to analyse will be a circular cavity whose internal flow is being driven by a shear layer along an arc of the circumference.

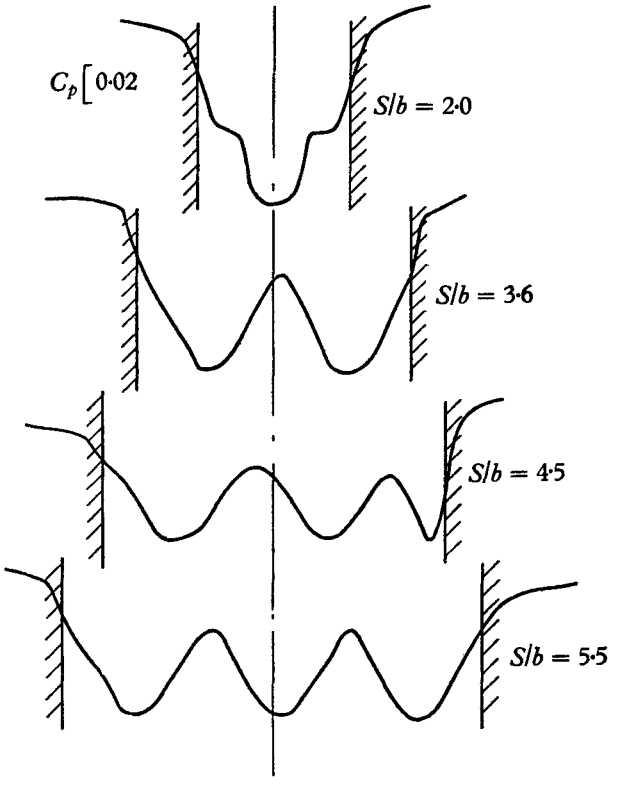

FIGURE 13. Pressure distribution along the span of a rectangular cavity for varying S/b, d/b = 0·5.

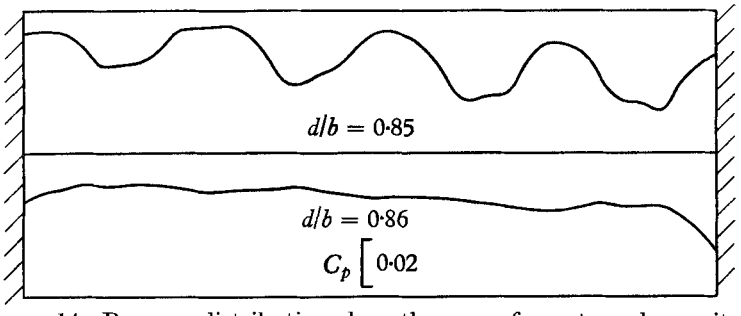

FIGURE 14. Pressure distribution along the span of a rectangular cavity with a rounded downstream corner for varying d/b, S/b = 9·0.

The span of the cavities could be varied from 10 to 8 in. by the insertion of wooden disks, and some of the resulting spanwise pressure distributions are shown in figure 15. For a value of d/b = 1·05 all configurations tested were steady and each produced a regular wave. The amplitude of the waves produced varied with

total span and a plot of this amplitude against s/b, figure 16, shows that a maximum is reached at about $s/b = 1{\cdot}27$.

The previous observations referring to a rectangular cavity for which $d/b = 0{\cdot}5$, showed that for a stable cell formation to exist s/b must lie within about $\pm 3\,\%$ of the preferred value, whereas the present tests show that a stable configuration can exist for variations of s/b up to at least $\pm 12\,\%$.

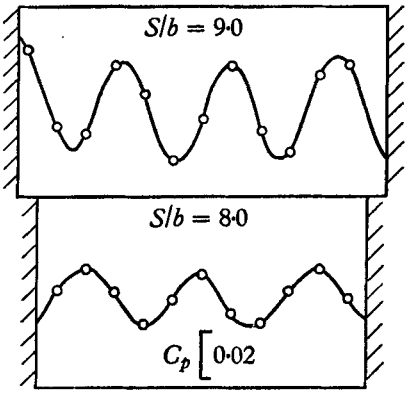

FIGURE 15. Pressure distribution along span of circular cavity for varying S/b, $d/b = 1{\cdot}05$.

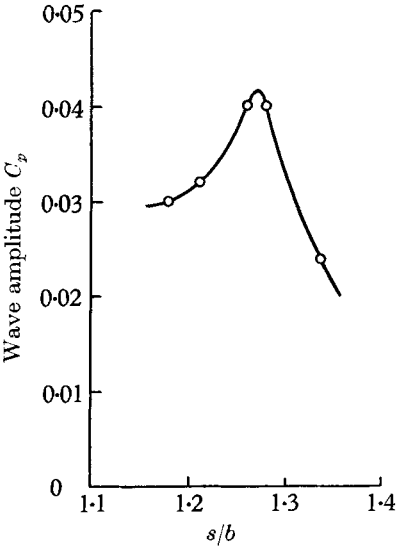

FIGURE 16. Amplitude of the waves of the spanwise pressure distribution against s/b for the circular cavity, $d/b = 1{\cdot}05$.

The pressure distributions for the circular cavity for which $d/b = 0{\cdot}42$ suffer from an insufficiency of pressure tappings, but nevertheless show that, although the variation of pressure coefficients reached a large amplitude of the order of 0·10, they were neither as regular nor as steady as in the previous case. The true value of s/b is uncertain but appears to be about 0·53.

8. Results

The main quantitative result that is drawn from the experiments conducted is a plot of the non-dimensional cell span s/b against the non-dimensional depth d/b. This is shown in figure 17 for all the previous experiments except that, as rounding the downstream corner had no effect on s/b when stable cell formations did appear, those results are not indicated. The points for the open rectangular cavities lie close to the straight line given by

$$s/b = 0{\cdot}6(1+d/b).$$

The points corresponding to the cavity with plates also lie near to this line. Also indicated are the regions during which the plain rectangular cavity apparently gave two-dimensional flow.

9. Discussion

The characteristics of the three-dimensional flow can be used to explain, at least in part, some effects found by both Roshko (1955) and Mills (1961). Both present graphs showing the variation of the static pressure at the downstream corner of the cavity against d/b, and although they differ in detail, which is not unexpected since Roshko used a cavity for which $S/b = 8{\cdot}0$, whereas for Mills's $S/b = 5{\cdot}0$, they are in broad agreement. They found that for values of d/b

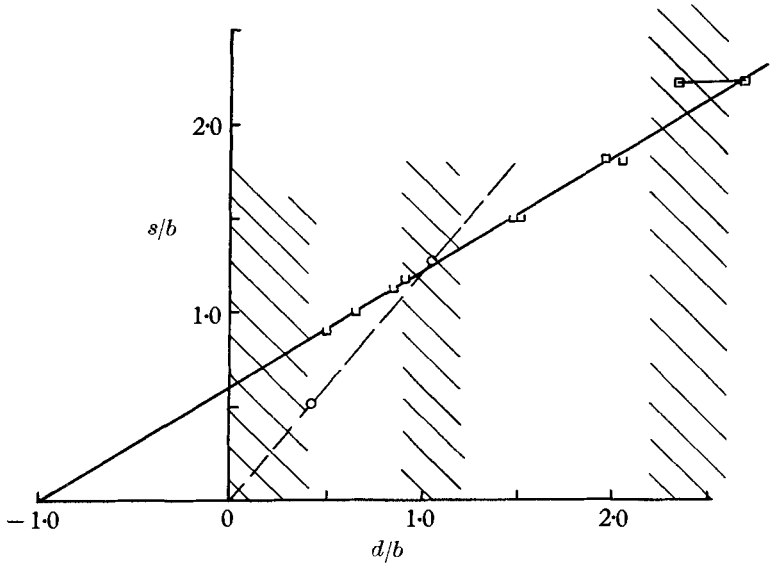

FIGURE 17. s/b against d/b for various cavities. Two-dimensional regions for open rectangular cavities shown cross-hatched. ⌊⌋ Rectangular cavities; □ rectangular with plates; ○ circular.

between about 0·45 and 0·85 the pressure varied with time and could take any value between two limits. It was in this region that it was found that, when d/b and S/b were not such as to produce regular cellular configurations, unsteady flow generally resulted. It is to be expected, however, that at a few values of d/b fairly stable pressure should have been present, but this was not observed.

The sharp change from intermittent to steady pressures, which occurred in Roshko's case at $d/b = 0{\cdot}87$, corresponds to the sudden collapse of the cellular flow found in our cavities at $d/b = 0{\cdot}875$ and $d/b = 0{\cdot}91$. The 'hysteresis' effect, which Roshko observed between about 1·2 and 1·8 and Mills between about 1·4 and 2·4, corresponds to the second region of cellular flow. The salient feature of this régime appears to be that the pressure can take either of two discrete values but cannot wander in between. This suggests that for each value of d/b there are two steady cellular configurations possible, which give different centre line pressure distributions. This was not observed to be the case for d/b between 1·25 and 1·52 when moving waves were produced. However, between 1·52 and 2·05 steady cellular conditions were observed and, as previously noted in connexion with figure 7, this could produce the observed hysteresis effect. The

remaining values of d/b which produced steady single values results correspond to the two-dimensional configurations shown in figure 17.

The effect of Reynolds number has not been investigated though, with the one exception previously mentioned, it was found that the steady cellular configurations did not change noticeably as the air speed was increased.

Further work is in progress to measure the unsteady pressures in these cavities.

REFERENCES

MILLS, R. D. 1961 *The Flow in Rectangular Cavities.* University of London, Ph.D. Thesis.

PLUMBLEE, H. E., GIBSON, J. S. & LASSITER, L. W. 1962 *Wright Patterson Air Force Base* WADD-TR-61-75.

ROSHKO, A. 1955 *Nat. Adv. Comm. Aero.*, Wash., Tech. Note, no. 3488.